

Chapter 8

Base Isolation for Earthquake-Resistant design

8.1 Introduction

A natural calamity like an earthquake has taken the toll of millions of lives through the ages in the unrecorded, and recorded human history. A disruptive disturbance that causes shaking of the surface of the earth due to underground movement along a fault plane or from volcanic activity is called earthquake. The nature of forces induced is reckless, and lasts only for a short duration of time. Yet, bewildered are the humans with its uncertainty in terms of its time of occurrence, and its nature. However, with the advances made in various areas of sciences through the centuries, some degree of predictability in terms of probabilistic measures has been achieved. Further, with these advances, forecasting the occurrence and intensity of earthquake for a particular region, say, has become reasonably adequate, however, this solves only one part of the problem to protect a structure - to know what's coming! The second part is the seismic design of structures - to withstand what's coming at it! Over the last century, this part of the problem has taken various forms, and improvements both in its design philosophy and methods have continuously been researched, proposed and implemented.

In this chapter, the concept of base isolation for earthquake-resistant design of the structures is presented. The modeling and analysis of multi-storey building, bridges and tanks supported on isolators is developed and demonstrated the effectiveness of seismic isolation.

8.2 Conventional Seismic Design Approach

Over the past few decades, earthquake resistant design of structures has been largely based on a ductility design concept worldwide. Looking at the Indian code specifically, the design philosophy evolve around the intensity of the earthquake: moderate earthquake or design basis earthquake (DBE) which has a 10% chance in a return period of 250 years, and most credible earthquake (MCE) which has a 2% chance in a return period of 250 years. The seismic philosophy in the Indian code expects the structure to possess a minimum strength to protect structural and non-structural contents for intensities less than DBE. For intensity equal to DBE, it should withstand without much structural damage, however, some non-structural damage is allowed, and for major earthquakes, it must not collapse suddenly. The

ductility helps to dissipate energy while undergoing large permanent deformations causing damage that can incur heavy repair costs, as much as building the structure itself. It is apparent from this approach that more emphasis is laid on life safety, and not much importance is given to protect the non-structural contents. Non-structural damage sometime costs more than the structure itself, for example, telecommunication data centers, nuclear facilities, laboratories etc. Hence, ductility arising from inelastic material behavior and detailing is relied upon in this philosophy.

Indian code follows the seismic coefficient method in determining the lateral design forces to build the structure. It is important to understand how the ductility is procedurally inculcated in this method. Seismic coefficient method helps to determine base shear considering only the fundamental mode of the structure. The performances of the intended ductile structures during major earthquake, however, have been proved to be unsatisfactory, and indeed far below expectation (Wang, 2002). High uncertainty of the ductility design strategy is primarily attributed to:

1. The desired strong-column weak-beam mechanism may not form in reality, due to existence of walls.
2. Shear failure of columns due to inappropriate geometrical proportions of short-column effect.
3. Construction difficulty in grouting, especially at beam-column joints, due to complexity of steel reinforcement required by ductility design.

Thus, it necessitates finding a method that is devoid of the shortcomings of the ductility approach. We shall see how the uncertainty in ductility design and the performance levels are increased in following section by an alternative and innovative approach.

8.3 Alternative and Emerging Approach: Base Isolation

We have seen that though ductile approach strives to tackle the effects of the earthquake, it had various shortcomings as discussed before. Base isolation is a passive control system; meaning thereby that it does not require any external force or energy for its activation. It is necessary to understand why base isolation is needed to enhance performance levels of the structure subjected to seismic excitations. To design structure in such a way, that it may withstand the actual force by fixed base structure elastically, is not feasible in two senses. First, the construction cost of the structure will be highly uneconomical. Second, if the overall strength of the structure is increased by making it more rigid, then it will be at the

expense of imparting actual ground forces to the structural contents, thus causing heavy non-structural damage.

Apparently, as the name implies base isolation tries to decouple the structure from the damaging effects of ground motion in the event of an earthquake. Base isolation is not about complete isolation of the structure from the ground, as with magnetic levitation, which may be very rarely practical. Most of the base isolation systems that have been developed over the years provide only 'partial' isolation. 'Partial' in the sense that much of the force transmitted, and the consequent responsive motions are only reduced by providing flexibility and energy dissipation mechanisms with the addition of base isolation devices to the structure.

Base isolation, as a strategy to protect structure from earthquake, revolves around a few basic elements of understanding:

1. **Period-shifting of structure:** Base isolator is a more flexible device compared to the flexibility of the structure. Thus, coupling both an isolator and the superstructure together increases the flexibility of the total isolated structural system. In this way, this technique lengthens the structures natural time period away from the predominant frequency of the ground motions, thus evading disastrous responses caused due to resonance.
2. **Mode of vibration:** The fundamental mode of vibration (first mode shape) is altered from continuous cantilever type structure to an almost rigid superstructure with deformations concentrated at the isolation level.
3. **Damping and cutting of load transmission path:** A damper or energy dissipater is used to absorb the energy of the force to reduce the relative deflection of the structure with respect to the ground.
4. **Minimum rigidity:** It provides minimum rigidity to low level service loads such as wind or minor earthquake loads.

Abundant literature is available on the base-isolated structures and their seismic performance (Kelly, 1986; Buckle and Mayes, 1990; Stanton and Roeder, 1991; and Ibrahim, 2008, Kelly and Jangid, 2001). It has been reported that several types of isolation systems were proposed by researchers and are being used in seismic isolation of structures (Jangid and Datta, 1995). The base isolation technique of protection of structures from earthquakes is also reported to be used for liquid storage tanks with different types of isolation systems (Shrimali and Jangid, 2002).

The isolation systems are also used nowadays in bridges as reported by Kunde and Jangid (2003). For bridges, earlier vertical mounting or bearings have been used widely; however, its primary uses have been for isolation of the vertical vibrations, and to control thermal stresses

due to expansion. With the advances in rubber technology in the 1980s, it became possible to produce bearings that had high vertical stiffness and low horizontal stiffness, thus enabling the concept of period-shifting and additional means of damping. However, with increasing flexibility the displacement response may get undesirable. This is where energy dissipater or damping is required. In elastomeric isolation systems, damping is provided by lead extrusion and in friction system, friction provides the means for energy dissipation. Figure 8.1 shows the effect of damping on acceleration response for various time periods. Such kinds of rubber based isolation systems are able to provide damping of the order of 10% to 15%.

In order to maintain vertical stiffness steel shims / plates are used which does not alter the horizontal flexibility. The two materials, namely rubber and steel, are vulcanized together resulting in elastomeric isolation systems. More details about isolation systems, their types, behavior and mathematical modeling will be dealt with in the subsequent topics.

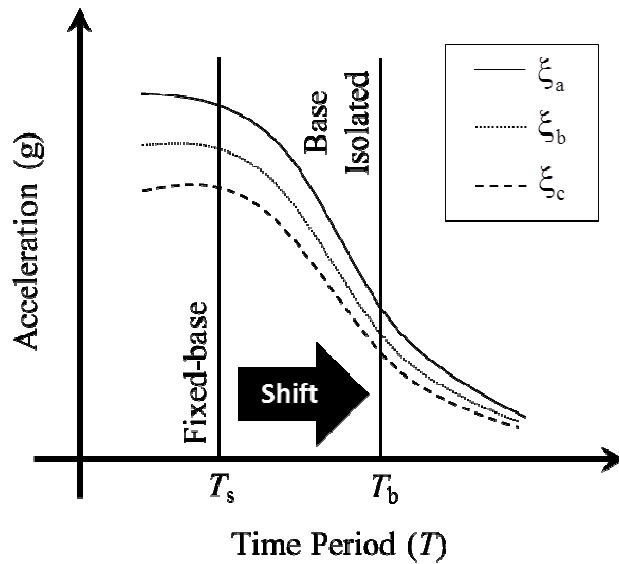


Figure 8.1 Idealized acceleration response spectrum ($\xi_a < \xi_b < \xi_c$).

Midrise structures with 10 to 15 stories are the most suitable to be base-isolated. Base isolation provides an excellent substitute for fixed base design where earthquakes are frequent. The economy of base isolation is not viewed in terms of its initial installment but over the design period of the structure during which it is expected to experience earthquake. After an event of earthquake, the repair of structure, and loss of non-structural components may be a more costly affair than installing base isolation. So far, base isolation technology has been adapted in very important structures such as hospitals, laboratories, and data centers etc. Also, base isolation has been found to be extremely useful for retrofitting of the old

structures where the aesthetic, architectural and heritage value is required to be maintained intact (Matsagar and Jangid, 2008).

In few countries located in high seismic zones, momentum of development and use of base isolation has increased over the years. New Zealand, United States, and Japan are the leading countries that have adopted this technology rapidly, and have put in great deal of energy and funds in this regard. Thus far no base-isolated buildings have been subjected to the designed earthquake motion to ascertain its ultimate capacity. It is worthwhile to mention that during the recent major earthquake in Tohoku, Japan some base-isolated structure had performed well within its limits (Takewaki, 2011). This will build confidence in the base isolation technology and its widespread use in routine constructions.

Though research has been going in this area during past 100 years, it was only since 1980s had base isolation been implemented following the modern engineering realms. Yet, a formalized and simple procedure for its implementation is not very well developed. The formalization through codes itself have been at the rudimentary level. Hopefully, with the simplified code procedures, construction techniques, and financial incentive (like lesser insurance premiums) earthquake protection can be a reality, and base isolation will gain popularity.

8.4 Elastomeric Base Isolation Systems

The developments in rubber technology made the base isolation a practical reality. In the implemented projects of base isolation worldwide, it is observed that elastomeric based systems are the most common. Typically, these systems consist of big rubber block, which can be natural or synthetic (in case of neoprene) that are generally characterized by high vertical stiffness compared to the horizontal stiffness and damping capacity. The vertical stiffness is kept close to rigid, as the structural members are designed to take care of the vertical force component of the seismic excitation. Providing high vertical stiffness also prevents undesirable bouncing motion that is induced if vertical flexibility is provided. Discussions on few popular base isolation systems are provided in the next sections.

8.4.1 Laminated Rubber Bearing

The laminated rubber bearings (LRB) represent the most commonly used elastomeric isolation system. The basic components of LRB are steel and rubber plates, built through vulcanization process in alternate layers (Simo and Kelly, 1984), as shown in Figure 8.2(a). The dominant feature of LRB is parallel action of linear spring and damping. A schematic

diagram for the mechanism is shown in Figure 8.2(b). Generally, the LRB is characterized with high damping capacity, horizontal flexibility and high vertical stiffness. The relatively low shear stiffness in the horizontal plane is provided by the rubber, and the high vertical stiffness is provided by steel shims to control the bouncing effect on the structure due to vertical vibration caused by the earthquake. The steel shims also help to confine the rubber from bulging out. The damping constant of the system varies considerably with the strain level of the bearing. The system operates by decoupling the structure from the horizontal components of the earthquake ground motion by interposing a layer of low horizontal stiffness between the structure, and its foundation. The isolation effects in this type of system are produced not by absorbing the earthquake energy, however by deflecting through the dynamics of the system. Usually, there is a large difference in the damping of the structure, and the isolation device, which makes the system non-classically damped.

The high-damping rubber bearings (HDRB) also exhibit similar properties, and falls in the same category of elastomeric systems (Kikuchi and Aiken, 1997; Koo et al., 1999; Tsopelas et al., 1991). The ideal force-deformation behavior of these isolation systems is generally represented by non-linear characteristics, as shown in Figure 8.2(c). The HDRB may exhibit hardening at higher strains values. However, the code specifies an equivalent linear viscous model (to be used for response spectrum analysis), which represents the linear stiffness with viscous damping.

Permanent residual displacement is very less in LRB after an event of earthquake as the rubber mobilizes sufficient restoring force required to re-position the building to its initial state. The restoring force F_b , can be mathematically modeled from the force-deformation plot as,

$$F_b = c_b \dot{x}_b + k_b x_b \quad (8.1)$$

where, c_b and k_b are damping and stiffness of the LRB, respectively.

The two parameters that characterize the LRB system are namely: (a) the isolation time-period T_b , and (b) damping ratio, ξ_b . Their specific values are obtained from the stiffness and damping for which the LRB is designed. These two parameters are defined as,

$$T_b = 2\pi \sqrt{\frac{M}{k_b}} \quad (8.2)$$

$$\xi_b = \frac{c_b}{2M \omega_b} \quad (8.3)$$

where, $M = (m_b + \sum_{j=1}^N m_j)$ is the total mass of the base-isolated building; m_j is the mass of j^{th} floor; and $\omega_b = 2\pi/T_b$ is the isolation frequency.

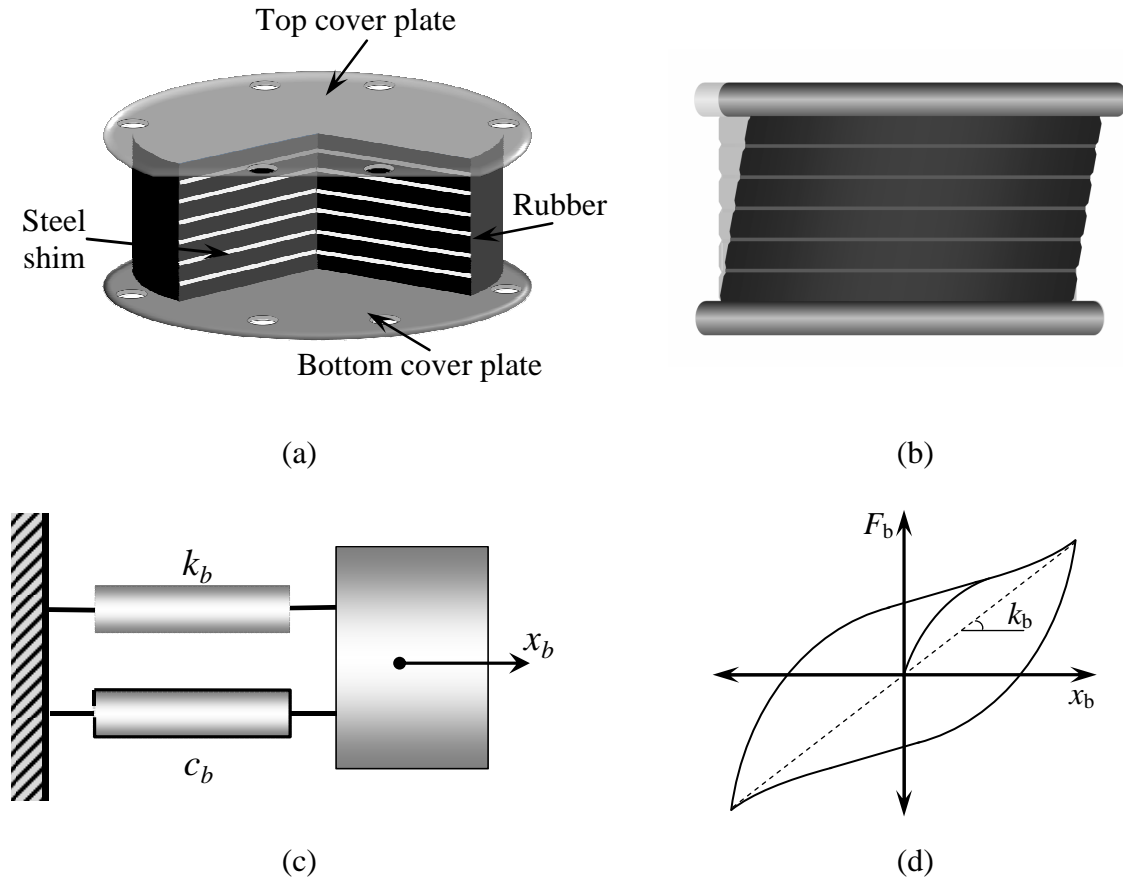


Figure 8.2 Laminated rubber bearing: (a) LRB; (b) Schematic diagram of LRB; (c) Force-deformation behavior of LRB.

The laminated rubber bearings generally exhibit linear force-deformation behavior (with some hardening effects at large strains i.e. 200 percent) and are characterized by their lateral stiffness and viscous damping ratio.

The vertical stiffness of the laminated rubber bearing is expressed by

$$K_v = \frac{E_c A}{t_r} \quad (8.4)$$

where A is the area of the bearing; t_r is the total thickness of rubber in the bearing; and E_c is the instantaneous compression modulus of the rubber-steel composites.

For a bearing square in plan the instantaneous compression modulus (Naeim and Kelly, 1999) is given by

$$E_c = 6.73S^2G \quad (8.5)$$

where S is the shape factor (i.e. ratio of the loaded area to the force-free area of the rubber layer); and G is the shear modulus of the bearing typically dependent on the rubber hardness.

For a bearing circular in plan the instantaneous compression modulus is given by

$$E_c = 6S^2G \quad (8.6)$$

The horizontal stiffness of the laminated rubber bearings is expressed by

$$K_h = \frac{GA}{t_r} \quad (8.7)$$

8.4.2 New Zealand Bearing

The second category of elastomeric bearings are lead-rubber bearings, which are similar to the LRB except that a central lead-core is used as in Figure 8.3(a), to provide additional means of energy dissipation, and initial rigidity against minor earthquakes and winds (Skinner et al., 1975; Robinson, 2000, Matsagar and Jangid, 2004, Jangid, 2010). Because this bearing is developed, and widely used in New Zealand, it is generally referred to as N-Z system. The lead-core provided, reduces the isolation level displacement by virtue of its energy absorbing capacity. The N-Z systems also provide an additional hysteretic damping through the yielding of the lead-core. This seismic isolation system provides the combined features of vertical load support, horizontal flexibility, restoring force and damping in a single unit. The schematic diagram of the combined mechanism is shown in Figure 8.3(b). The ideal force-deformation behavior of the N-Z system is generally represented by non-linear characteristics following a hysteretic nature as shown in Figure 8.3(c).

The N-Z system also poses the capability of mobilizing the restoring force as LRB. However, the mathematical modeling is done with the help of a non-linear model (Wen, 1976) to characterize the hysteretic behavior of the N-Z systems. The restoring force developed in the isolation bearing is given by,

$$F_b = c_b \dot{x}_b + \alpha k_b x_b + (1 - \alpha) F_y Z \quad (8.8)$$

where, F_y is the yield strength of the bearing; α is an index which represent the ratio of post to pre-yielding stiffness; k_b is the initial stiffness of the bearing; c_b is the viscous damping of the bearing; and Z is the non-dimensional hysteretic displacement component satisfying the following non-linear first order differential equation expressed as,

$$q\dot{Z} = A\dot{x}_b + \beta|\dot{x}_b|Z|Z|^{n-1} - \tau\dot{x}_b|Z|^n \quad (8.9)$$

where, q is the yield displacement; dimensionless parameters β , τ , A and n are selected such that predicted response from the model closely matches with the experimental results. The parameter n is an integer constant, which controls smoothness of transition from elastic to plastic response.

The N-Z system is characterized by three parameters: (a) isolation period T_b , (b) damping ratio ξ_b and (c) normalized yield strength i.e. F_y/W (where, $W=Mg$ is the total weight of the building; and g is the acceleration due to gravity). The bearing parameters T_b and ξ_b are computed by equations (8.2) and (8.3).

In the above equation, post-yield stiffness of the bearing is used. The typical values of parameters of the N-Z system are $q = 2.5$ cm, $\beta = \tau = 0.5$, $A = 1$ and $n = 2$.

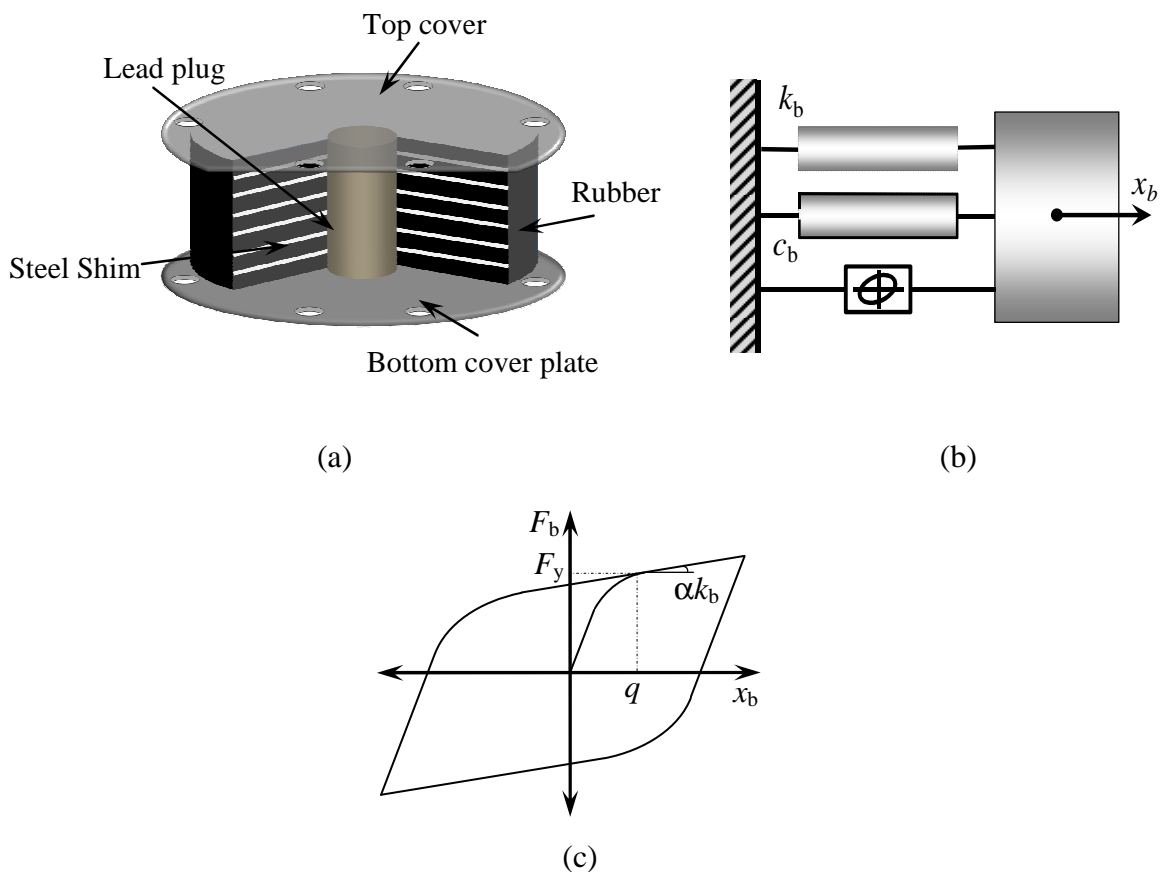


Figure 8.3 New Zealand bearing: (a) N-Z; (b) Schematic diagram of N-Z; (c) Force-deformation behavior of N-Z.

Example 8.1

Determine the horizontal and vertical stiffness of square (300mm×300mm) and circular (diameter = 300mm) bearing as shown in the Figure 8.4. The height of the bearing between top and bottom steel plates is 75mm. The five number of 5mm thick steel plates are provided in the bearings. Take the shear modulus of the rubber as 1.06 N/mm².

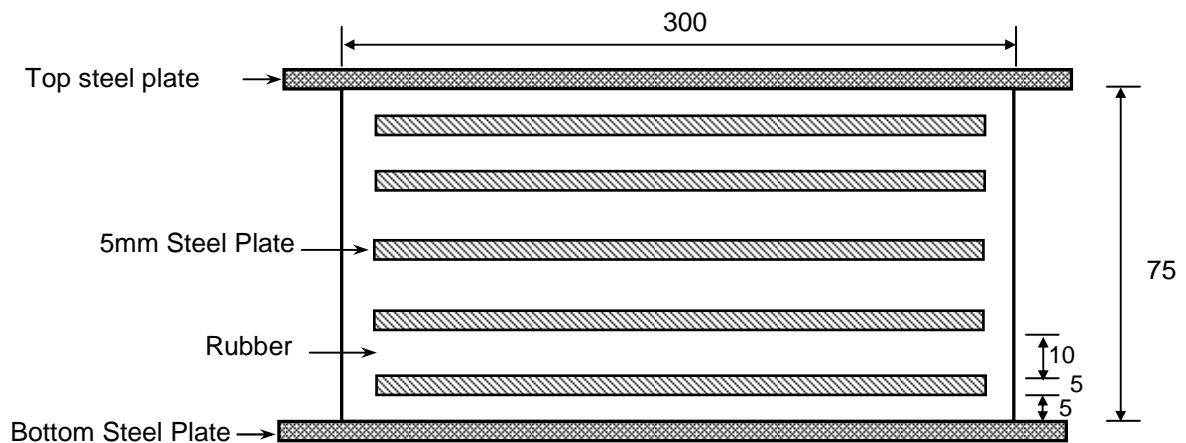


Figure 8.4 Cross-section of the bearing (all dimension in mm).

Solution: Given for the each bearing

Total thickness of the rubber = $75 - 5 \times 5 = 50$ mm

The shear modulus, $G = 1.06$ N/mm²

(a) Square Bearing

The shape factor, $S = \frac{300}{2 \times 15} = 10$

$$E_c = 6.73 \times 10^2 \times 1.06 = 713.4 \text{ N/mm}^2$$

$$K_v = \frac{713.4 \times (300 \times 300)}{50} = 1284120 \text{ N/mm}$$

The horizontal stiffness of the bearing

$$K_h = \frac{1.06 \times 300 \times 300}{50} = 1908 \text{ N/mm}$$

(b) Circular Bearing

The shape factor, $S = \frac{300}{2 \times 15} = 10$

$$E_c = 6 \times 10^2 \times 1.06 = 636 \text{ N/mm}^2$$

$$K_v = \frac{636 \times \left(\frac{\pi}{4} \times 300 \times 300\right)}{50} = 899123.8 \text{ N/mm}$$

The horizontal stiffness of the bearing

$$K_h = \frac{1.06 \times \left(\frac{\pi}{4} \times 300 \times 300\right)}{50} = 1498.5 \text{ N/mm}$$

8.5 Sliding Base Isolation Systems

Sliding systems with restoring force offers advantages over elastomeric isolation systems. The sliding system is effective in the sense that it is capable of taking care of wide range of frequency input from the seismic excitation. The frictional force is proportional to the mass of the structure and hence the center of mass and the center of resistance of the sliding support coincide, thus diminishing the torsional effects produced by asymmetric building.

8.5.1 Pure Friction System

The simplest sliding isolation system, used popularly for bridges in particular, is the pure friction (P-F) system based on the mechanism of sliding friction (Westermo and Udawadia, 1983) as shown in Figure 8.5(a). The use of layer of sand or roller in the foundation of the building is the example of P-F base isolator. Under normal conditions of ambient vibrations, and small magnitude earthquakes, the system acts like a fixed base system due to the static frictional force. For large earthquake, the static value of frictional force is overcome, and sliding occurs with reduced dynamic resistance thereby reducing the accelerations. The horizontal frictional force at the bearing interface offers resistance to the motion, and dissipates energy. The schematic and force-deformation behavior of P-F system is rigid elastic-plastic as shown respectively in Figure 8.5(b) and 8.5(c). It should be noted that the coefficient of friction μ of P-F system varies significantly with the nature of friction surface used. Generally, in addition to these types of bearings supplemental devices are indispensable to provide restoring capacity, and check on the excessive displacements across isolation layers. Coulomb's frictional resistance is used to model the limiting frictional force. It is to be noted that the frictional coefficient μ is independent of the sliding velocity. The limiting frictional force in the bearing is given by,

$$F_s = \mu Mg \quad (8.10)$$

Depending upon the magnitude of the frictional force, F_x the system will be in stick or slip conditions. If $F_x < F_s$, then it will be in non-sliding (stick) phase, and the bearing force, F_b is,

$$F_b = F_x \quad (8.11)$$

If $F_x > F_s$, then it will be in sliding (slip) phase with bearing force, F_b as,

$$F_b = F_s \operatorname{sgn}(\dot{x}_b) \quad (8.12)$$

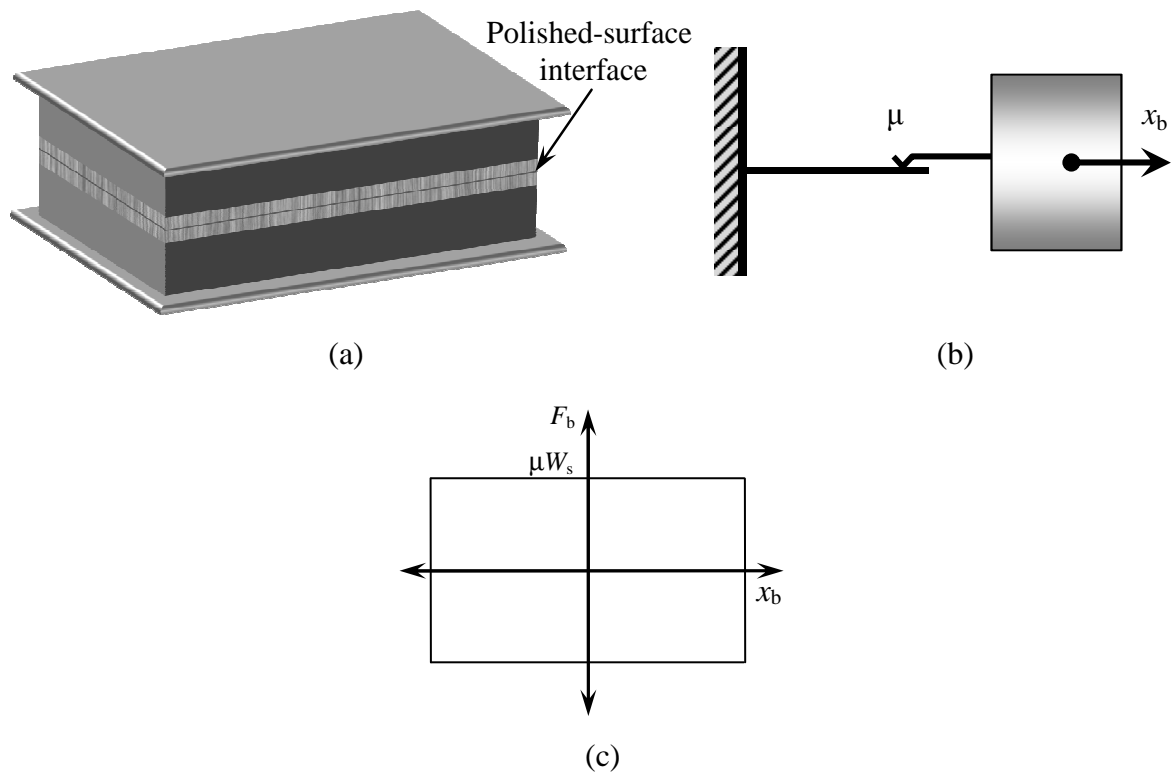


Figure 8.5 Pure friction system: (a) P-F; (b) Schematic diagram of P-F; (c) Force-deformation behavior of P-F.

8.5.2 Friction Pendulum System

One of the most popular and effective techniques for seismic isolation is through the use of sliding isolation devices. The sliding systems exhibit excellent performance under a variety of severe earthquake loading and are very effective in reducing the large levels of the superstructure acceleration. These isolators are characterized by their insensitivity to the frequency content of earthquake excitation, because of the tendency of sliding system to reduce and spread the earthquake energy over a wide range of frequencies. There is another advantage of sliding isolation systems over conventional rubber bearings. Due to development of the frictional force at the base, it is proportional to the mass of the structure, and the center of mass and center of resistance of the sliding support coincides. Consequently, the torsional effects produced by the asymmetric building are diminished.

The concept of sliding bearings is combined with the concept of a pendulum type response, resulting in a conceptually interesting seismic isolation system known as a friction pendulum system (FPS) (Zayas et al., 1990) as shown in Figure 8.6(a). A simple pendulum type response model is shown in Figure 8.6(b) to illustrate the similarity to friction pendulum system. The concept of sliding systems is marked by sliding of an articulated slider on

spherical concave chrome surface. The slider is faced with a bearing material which when in contact with the polished chrome surface results in development of friction force while concave surface produces restoring force. The system is activated only when the earthquake forces overcome the static value of friction and coefficient of friction depends upon the velocity attained. The FPS develops a lateral force equal to the combination of the mobilized frictional force, and the restoring force that develops because of the rising of the structure along the spherical concave surface (Jangid, 2005). The combined mechanism of FPS system, and its ideal force-deformation behavior is shown in Figure 8.6(c) and 8.6(d), respectively.

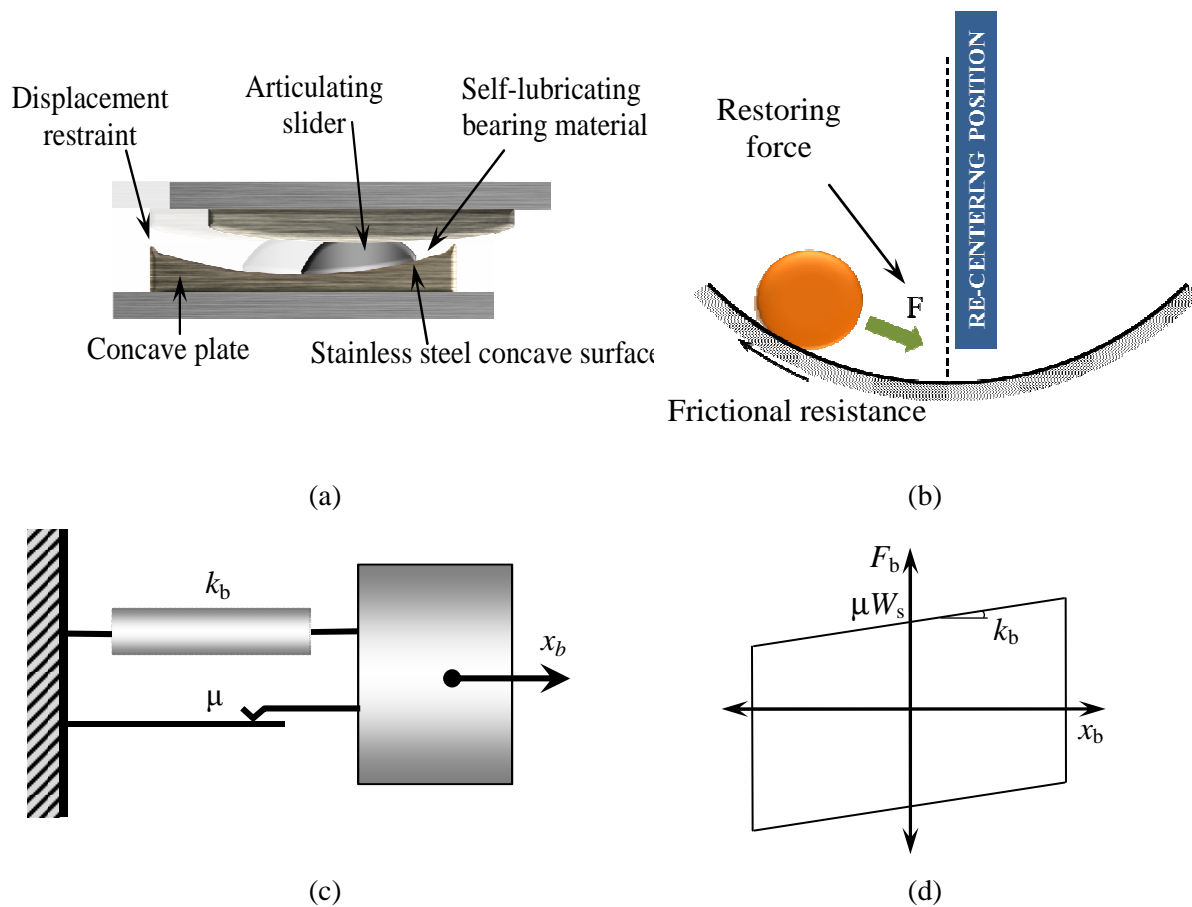


Figure 8.6 Friction pendulum system: (a) FPS; (b) Pendulum action; (c) Schematic diagram of FPS; (d) Force-deformation behavior of FPS.

The resisting force provided by the system can be mathematically modeled as,

$$F_b = k_b x_b + F_x \tag{8.13}$$

where, k_b is the bearing stiffness provided by virtue of inward gravity action at the concave surface, and F_x is the frictional force.

The system is characterized by two parameters: (a) bearing isolation period T_b that

depends upon radius of curvature of concave surface, and (b) friction coefficient μ . The isolation stiffness k_b is adjusted such that the specified value of the isolation period evaluated by equation (8.2).

8.5.3 Resilient-Friction Base Isolation System

Resilient-friction base isolator (R-FBI) system consists of concentric layers of Teflon-coated plates in friction contact with each other, and a central rubber core (Mostaghel and Khodaverdian, 1987; Mostaghel and Mortazavi, 1991) as shown in Figure 8.7(a). It combines the beneficial effect of damping provided through friction, and the resiliency of the rubber. The rubber core distributes the sliding displacement, and velocity along the height of the R-FBI. The rubber does not carry any vertical loads, and are vulcanized to the sliding ring. The system provides isolation through the parallel action of friction, damping, and restoring force.

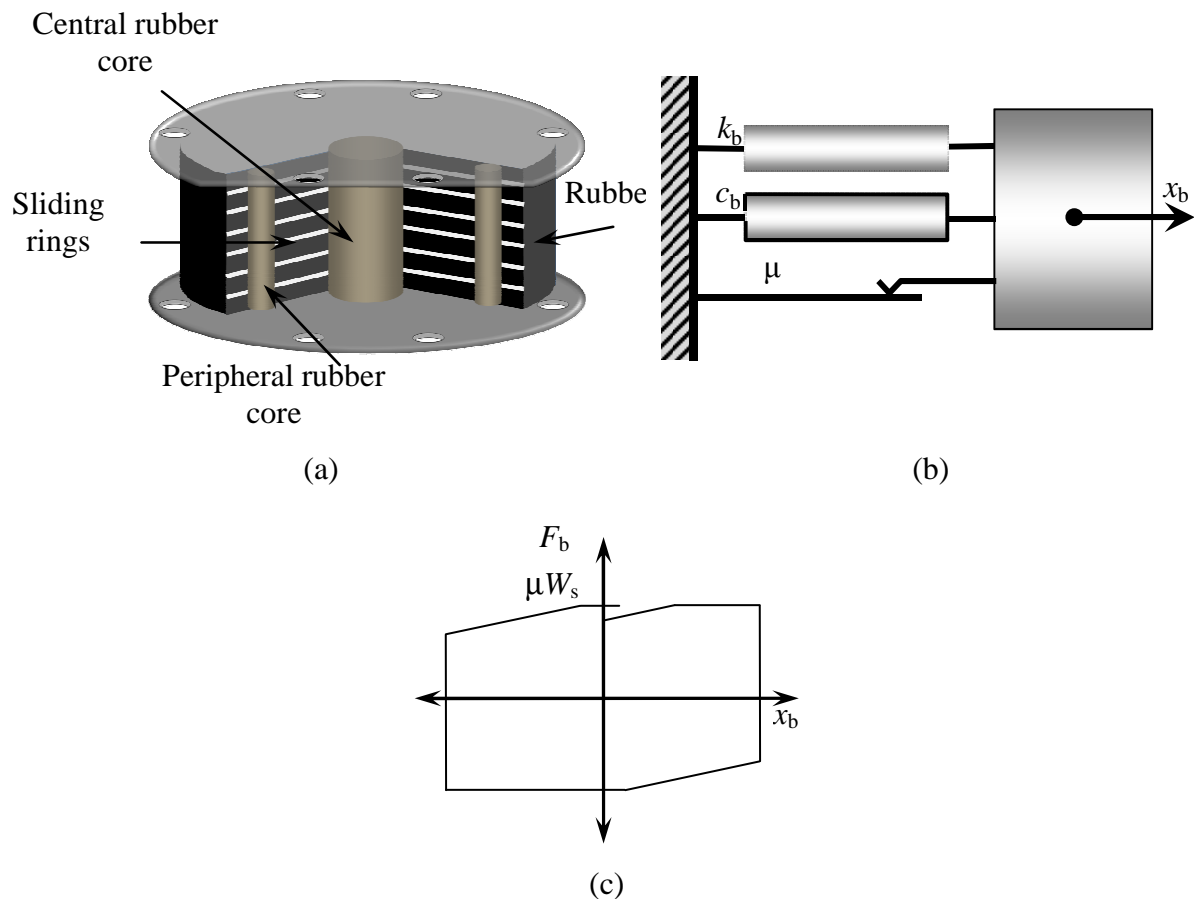


Figure 8.7 Resilient friction base isolation system: (a) R-FBI; (b) Schematic diagram of R-FBI; (c) Force-deformation behavior of R-FBI.

A schematic diagram of the mechanism is shown in Figure 8.7(b) As the R-FBI is very rigid in the vertical direction it does not provide isolation against vertical ground motion. The

ideal force-deformation characteristic of R-FBI is as shown in Figure 8.7(c) along with the schematic diagram. The bearing force in case of R-FBI system is,

$$F_b = c_b \dot{x}_b + k_b x_b + F_x \quad (8.14)$$

Thus, the parameters, defining behavior of R-FBI, are (a) the isolation period T_b , (b) damping ratio ξ_b , and (c) friction coefficient μ . The T_b and ξ_b are evaluated respectively from equations (8.2) and (8.3).

8.5.4 Electricite-de-France System

This system was developed under the auspices of “Electric de France” (EDF) standardized for nuclear power plants in region of high seismicity (Gueraud, 1985). The EDF base isolator consists of laminates (steel reinforced) of neoprene pad topped by lead-bronze plate which is in friction contact with steel plate anchored to the base-raft of the structure as shown in Figure 8.8(a). The EDF base isolator essentially uses elastomeric bearing and friction plate in series. An attractive feature of EDF isolator is that for lower amplitude ground excitations, the lateral flexibility of neoprene pad provides seismic isolation, and at high level of excitation sliding will occur which provides additional protection. Such dual isolation technique was intended for small earthquakes where the deformations are concentrated only at the bearings. However, for larger earthquakes the bronze and steel plates are used to slide, and dissipate seismic energy. The conceptual schematic model, and force deformation behavior of EDF isolator is shown in Figure 8.8(b) and 8.8(c), respectively.

The restoring force F_b from the force-deformation behavior can be mathematically modeled as,

$$F_b = c_b \dot{x}_b + k_b x_b \quad (8.15)$$

When the restoring force exceeds the limiting frictional force F_s the sliding at the top plate of the EDF system takes place. The restoring force during the sliding phase remains constant and is given by,

$$F_b = F_s \operatorname{sgn}(\dot{x}_b) \quad (8.16)$$

Thus, the EDF system is characterized by the parameters: (a) isolation period T_b , (b) damping ratio ξ_b , and (c) friction coefficient of top plate μ .

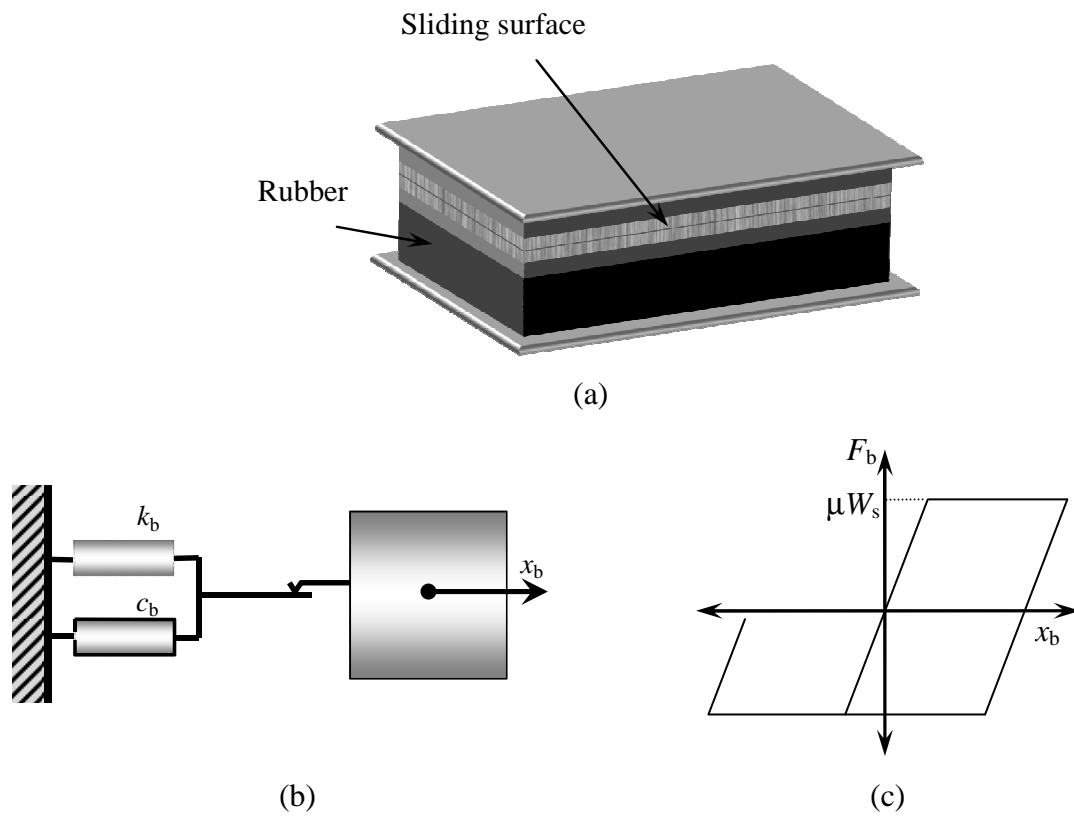


Figure 8.8 Electricite-de-France system: (a) EDF; (b) Schematic diagram of EDF; (c) Force-deformation behavior of EDF.

8.6 Modeling and Analysis of Base-Isolated Buildings

Buildings are places of dwelling and work. Buildings occupy people and for a good duration of time. The destruction of buildings in an earthquake can result in both heavy casualties and economic damage, which is evident from previous such catastrophic events. So these must be many of the structures that require earthquake protection. In this section, we analyze simple building in 2D plane as shear type building model subjected to understand its dynamic responses when subjected to earthquake excitation. It should be emphasized that the accuracy of a solution of any problem depends upon how closely the model simulates the exact behavior of a real-life structure. However, any assumption to simplify the complex models to decrease the computational cost and time to obtain sufficiently accurate results is welcome.

8.6.1 Assumptions

1. The superstructure is considered to remain within the elastic state during the period of seismic excitation. This assumption is considered appropriate because the base isolation attempts to reduce the earthquake response keeping it within the elastic state.
2. The floors are assumed to be rigid in its plane, and the mass is assumed to be lumped at each floor level.
3. The columns are inextensible and weightless, providing lateral stiffness, which governs superstructure time period of the structure.

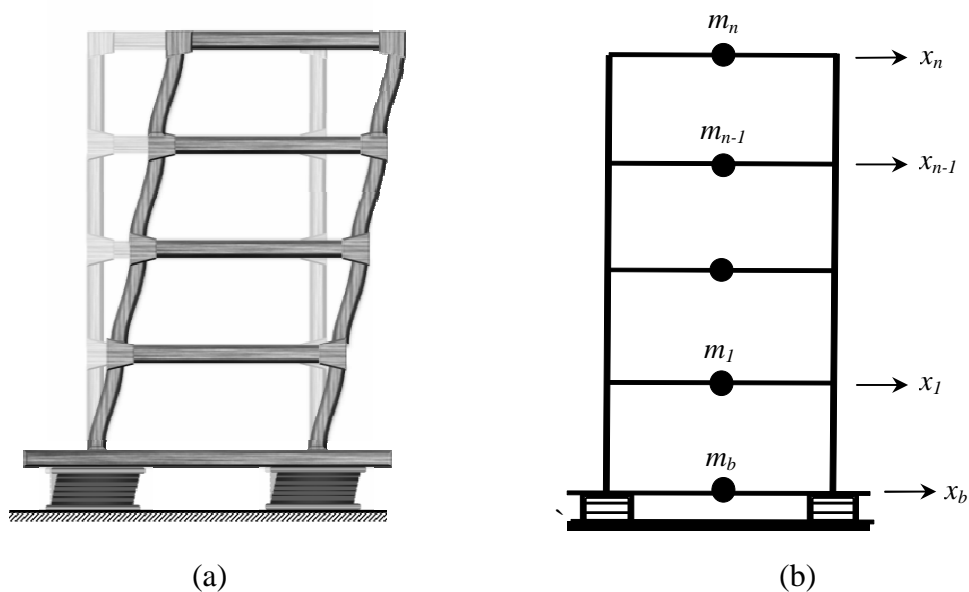


Figure 8.9 Building model: (a) Assumed deformed shape; (b) Lumped mass model.

8.6.2 Governing Equations of Motion

For a multi-storied building, an assumed deformation profile is shown in Figure 8.9(a). The columns in the model is assumed to undergo shear deformation and floor diaphragm, being relatively more rigid than the columns, do not bend or undergo axial deformation under earthquake excitation. Therefore degrees of freedom x_i corresponds to floor level lumped with mass m_i in the horizontal plane. The displacement across the isolation (isolator displacement) is denoted by x_b . Generally, the displacements of floors are expressed relative to the base mass / slab, whereas the displacement of the base mass is expressed relative to the ground.

A mathematical model of a base-isolated building with a base slab, resting over the isolator device, is shown in Figure 8.9(b). Under the most ideal conditions, this model holds good. However, all the isolators may not have the same force-deformation behavior, hence even for unidirectional forcing there maybe three motions. The restoring actions to these motions are provided by the isolators. Before formulating the necessary equations of motion, the dynamic degrees of freedom are chosen as shown in Figure 8.10 when dissimilar isolators are provided.

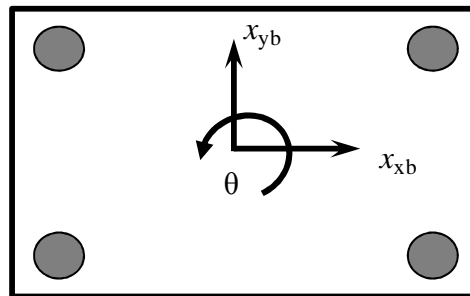


Figure 8.10 Dynamic degrees of freedom of base mass or slab.

The equation of motion for the superstructure placed over the base slab under seismic excitation takes the form as follows,

$$[M_s]\{\ddot{x}_s\} + [C_s]\{\dot{x}_s\} + [K_s]\{x_s\} = -[M_s]\{r\}(\ddot{x}_b + \ddot{x}_g) \quad (8.17)$$

where, $[M_s]$, $[C_s]$ and $[K_s]$ are the mass, damping, and stiffness matrices of the superstructure, respectively; $\{x_s\}$, $\{\dot{x}_s\}$ and $\{\ddot{x}_s\}$ are the unknown relative displacement, velocity, and acceleration vectors of each floor level with respect to the base slab,

respectively; \ddot{x}_b and \ddot{x}_g are the base slab and earthquake ground acceleration, respectively, and $\{r\}$ is the vector of influence coefficient.

The equation of motion for the base mass under seismic excitation is given by,

$$m_b \ddot{x}_b + F_b - k_1 x_1 - c_1 \dot{x}_1 = m_b \ddot{x}_g \quad (8.18)$$

where, m_b is the base slab mass; x_1 and \dot{x}_1 are the first floor displacement and velocity respectively; k_1 and c_1 is the damping and stiffness of the first floor of the superstructure, respectively, and F_b is the restoring force of the base isolator. Equations (8.15) and (8.16) can be coupled, and written as,

$$[M]\{\ddot{x}\} + [C]\{\dot{x}\} + [K]\{x\} + [D]\{F_b\} = -[M]\{r\}(\ddot{x}_g) \quad (8.19)$$

where, $[D]$ is the location matrix of the isolator.

The response of the base-isolated building can be obtained by solving the equation (8.19) using the step-by-step Newmark's Beta method given in the Section 7.5.

Example 8.2

Consider a five-storey building having the fundamental time period of the superstructure be 0.5 sec and damping of the order of 2 percent. The building has the same inter-storey stiffness at all floors. The masses at all the floors as well as base mass are also same. Two base isolation systems are designed for this building namely: (i) LRB system with characteristics as $T_b = 2$ sec and $\xi_b = 10$ percent and (ii) FPS system with $T_b = 2$ sec and $\mu = 0.05$. Determine the top floor absolute acceleration of the superstructure (i.e. $\ddot{x}_a = \ddot{x}_n + \ddot{x}_b + \ddot{x}_g$) and the relative base displacement (x_b). Also, compare the results for fixed base condition.

Solution:

The response building to El-Centro, 1940 earthquake ground motion is shown in Figures 8.11 and 8.12 for LRB and FPS system, respectively. Figures show that there is significant reduction in the absolute acceleration of superstructure for both models confirming the effectiveness of base isolation in reducing the seismic response of structures. The maximum isolator displacement is observed to be 12.34cm and 7.11cm for LRB and FPS system, respectively.

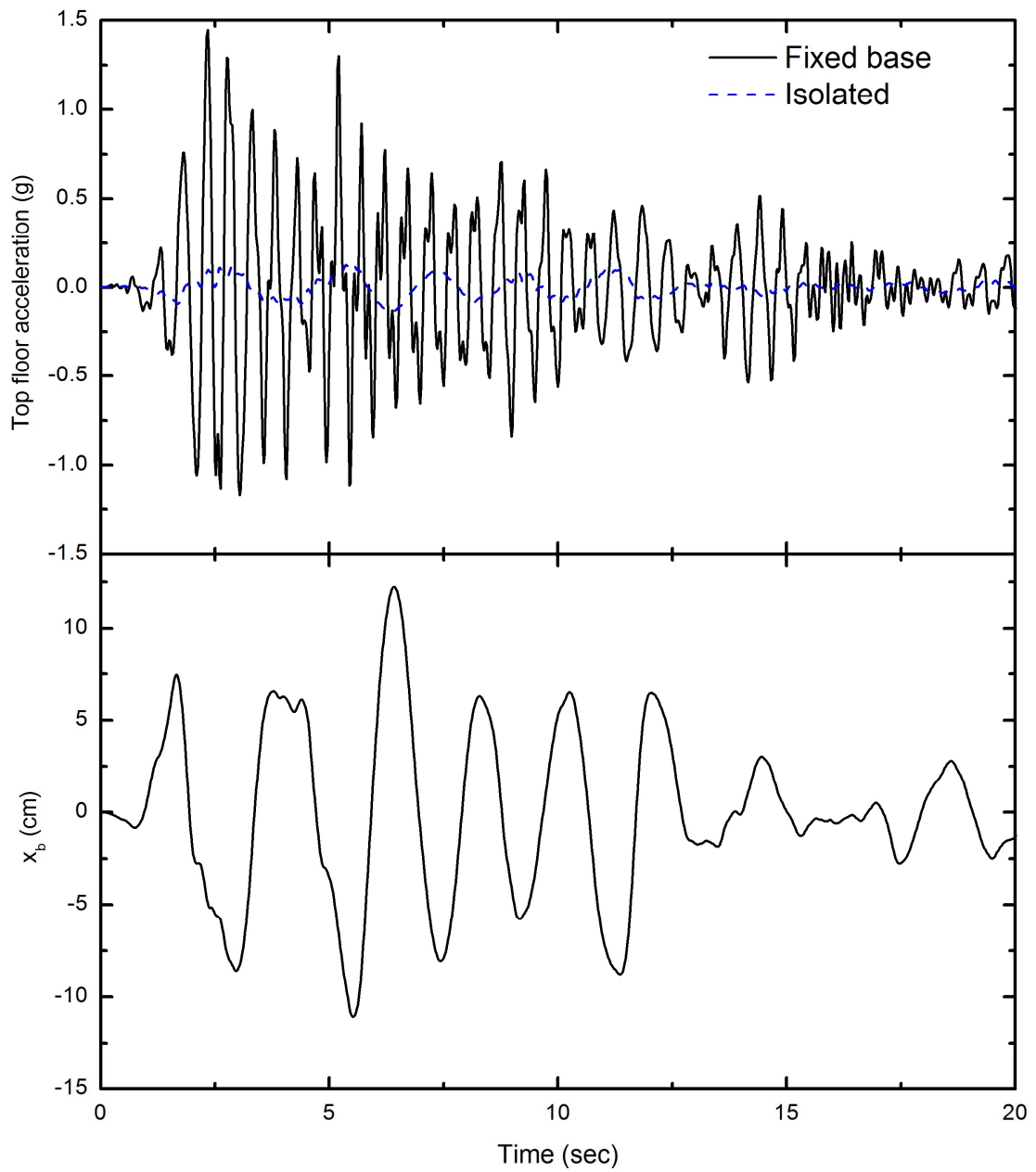


Figure 8.11 Response of a five-storey building isolated by LRB system.

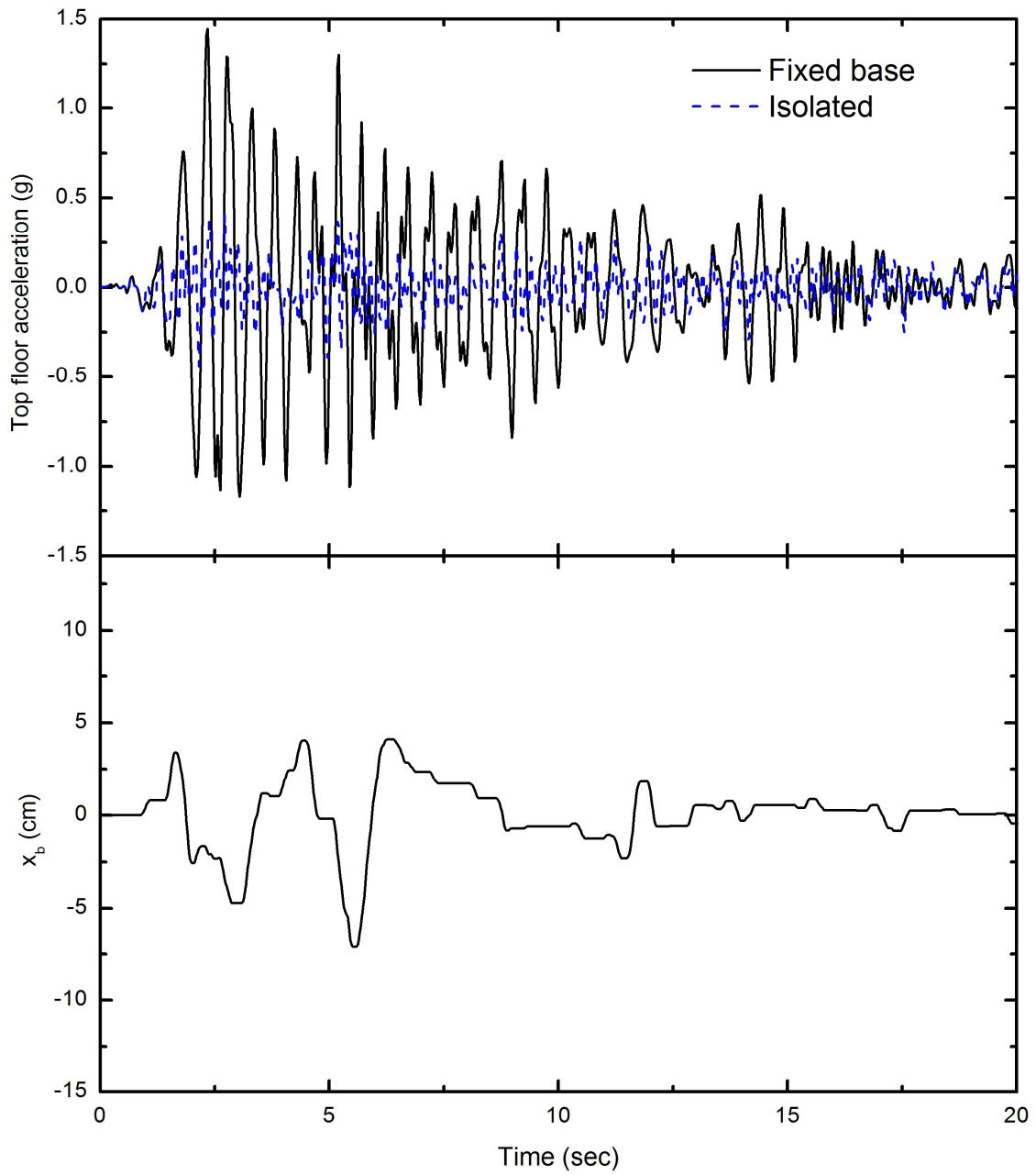


Figure 8.12 Response of a five-storey building isolated by FPS system.

8.7 Modeling and Analysis of Base-Isolated Bridges

Like buildings, bridges also need to be protected from earthquake events. Bridges are lifeline structures and require seismic design, why so, because they provide the necessary transportation network which is critical to conducting emergency relief and rehabilitation for post-earthquake operations. Thus, dynamic assessment should carefully be taken into account while designing bridges. In this, section a 3D three-span continuous deck bridge, as shown in Figure 8.13, subjected to earthquake excitation is analyzed (refer Kunde and Jangid, 2003,2006, Jangid, 2004, Jangid, 2008).

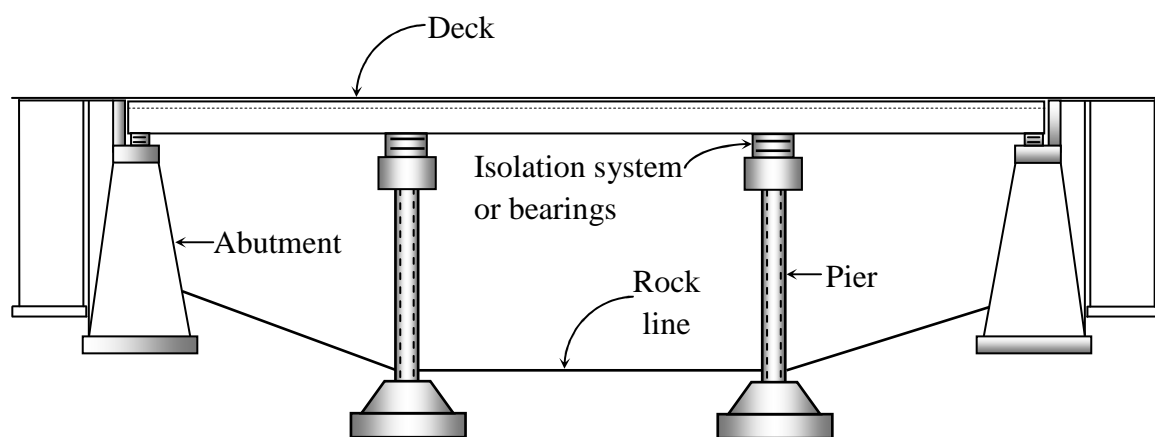


Figure 8.13 Model of three-span continuous girder bridge

8.7.1 Assumptions

1. Bridge superstructure and piers are assumed to remain in the elastic state during the earthquake excitation. This is a reasonable assumption as the isolation attempts to reduce the earthquake forces in such a way that the structure remains within the elastic range.
2. Piers of the bridge are fixed at the foundation level and effects of soil-structure interaction are ignored. The abutments of the bridge are assumed as rigid.
3. The bridge is founded on firm soil or rock and the earthquake excitation is perfectly correlated at all supports.
4. The base isolation system provided at the piers and abutments have the same dynamic characteristics.
5. The bridge deck and piers are modeled as a lumped mass system assumed to be divided into number of small discrete elements.

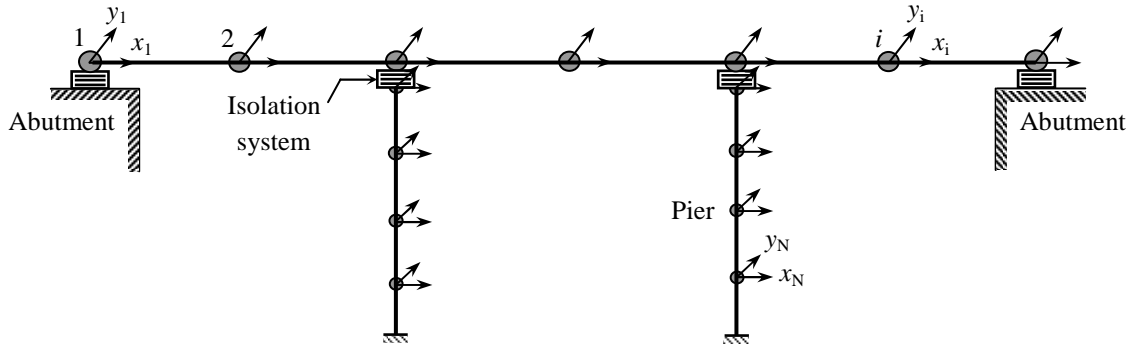


Figure 8.14 Lumped mass bridge model

8.7.2 Governing Equations of Motion

The structure is discretized along the length of the deck with masses lumped at abutments and intermediate supports, and at mid-spans as shown in Figure 8.14. Also, structure is discretized and masses are lumped along the pier. Each lumped mass m_i corresponds to a node i , which has two degree of freedom- one in longitudinal direction x_i and other, in transverse direction y_i of the deck.

The equation of motion of the isolated bridge system under the horizontal component of earthquake ground motion is expressed in the following matrix form,

$$[M]\{\ddot{z}\} + [C]\{\dot{z}\} + [K]\{z\} = -[M]\{r\}\{\ddot{z}_g\} \quad (8.20)$$

$$\{\ddot{z}_g\} = \begin{Bmatrix} \ddot{x}_g \\ \ddot{y}_g \end{Bmatrix} \quad (8.21)$$

where $[M]$, $[K]$ and $[C]$ represents the mass, stiffness and damping matrices, respectively of the isolated bridge system; $\{\ddot{z}\}$, $\{\dot{z}\}$ and $\{z\}$ represent the structural acceleration, structural velocity and structural displacement vectors, respectively; $\{r\}$ is the influence coefficient matrix; $\{\ddot{z}_g\}$ is the earthquake acceleration vector; \ddot{x}_g and \ddot{y}_g are the earthquake ground accelerations acting in the longitudinal and transverse direction of the bridge, respectively. The damping matrices of the bridge deck and piers are not explicitly known. These are constructed from assumed modal damping in each mode of vibration using its mode-shapes and frequencies.

The response of the base-isolated bridge can be obtained by solving the equation (8.20) using the step-by-step Newmark's Beta method given in the Section 7.5.

The stiffness of the bearings is obtained by the following expression

$$T_b = 2\pi \sqrt{\frac{m_d}{\sum k_b}} \quad (8.22)$$

where m_d is the mass of the bridge deck; $\sum k_b$ is the sum of the horizontal stiffness of all the bearings provided for bridge isolation; and T_b is the isolation time period of the bearings. Note that the T_b may be interpreted as the fundamental time period of the isolated bridge if the deck and piers of the bridge are perfectly rigid. However, the flexibility of the bridge deck and piers will slightly increase the fundamental time period of the bridge beyond the T_b .

The total viscous damping of the elastomeric bearings is expressed as

$$c_b = 2\xi_b m_d \omega_b \quad (8.23)$$

where c_b is total viscous damping of all the bearings; ξ_b is the damping ratio of the elastomeric bearings; and $\omega_b = 2\pi/T_b$ is the isolation frequency of the bearings.

Example 8.3

Consider a three-span continuous bridge with properties of the deck and piers given below.

Properties	Deck	Piers
Cross-sectional area (m ²)	3.57	4.09
Moment of inertia as (m ⁴)	2.08	0.64
Modulus of elasticity (N/m ²)	25×10 ⁹	25×10 ⁹
Mass density (kg/m ³)	2.4×10 ³	2.4×10 ³
Length/height (m)	3@30 = 90	8

The bridge is isolated using the elastomeric bearings with $T_b = 2$ sec and $\xi_b = 12.5\%$. Determine the absolute acceleration at the center of bridge deck, base shear in the piers and the relative displacement of the elastomeric bearings at the abutment and piers under El-Centro, 1940. The N-S component is applied in the longitudinal direction and other orthogonal component with scaling factor of 1.6 is applied in the transverse direction.

Solution:

Based on the method developed in the Section 8.7, the computer program in the FORTRAN was written and the response of the bridge to El-Centro, 1940 earthquake ground motion is shown in Figures 8.15 and 8.16 in the longitudinal and transverse direction, respectively. Figures show that there is significant reduction in the absolute acceleration of deck and base shear in the piers. The maximum response of the bridge is summarized below:

Response quantity	Longitudinal	Transverse
Deck acceleration of non-isolated bridge (g)	0.905	0.985
Deck acceleration of isolated bridge (g)	0.150	0.219
Reduction in deck acceleration (%)	83.42	77.76
Pier base shear of non-isolated bridge (W)	0.492	0.541
Pier base shear of isolated bridge (W)	0.079	0.120
Reduction in pier base shear (%)	83.94	77.81
Displacement of bearing at abutment (cm)	14.67	21.41
Displacement of bearing at pier (cm)	13.91	20.37

($W = m_d g =$ weight of the bridge deck)

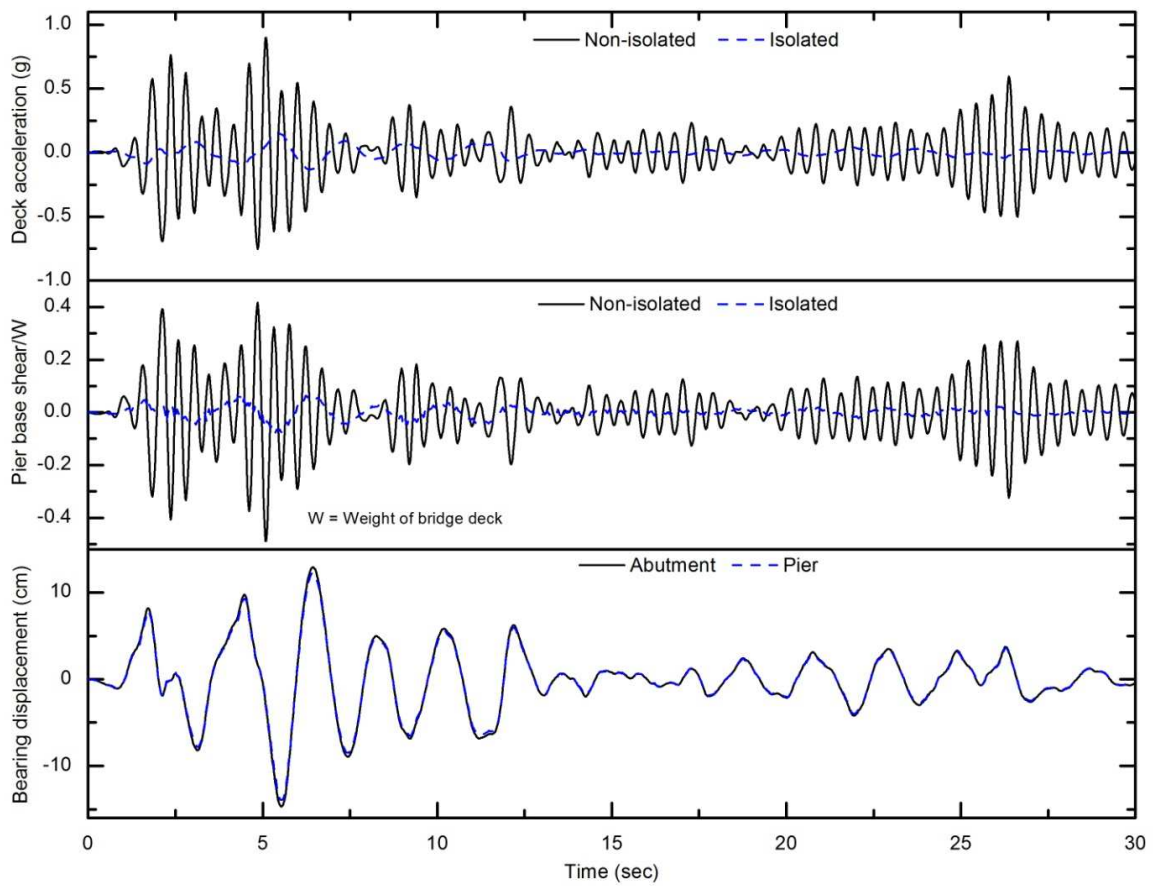


Figure 8.15 Time variation of the absolute deck acceleration, base shear in piers and bearing displacements in the longitudinal direction of the bridge to El-Centro, 1940 earthquake excitation ($T_b = 2$ sec and $\xi_b = 12.5\%$).

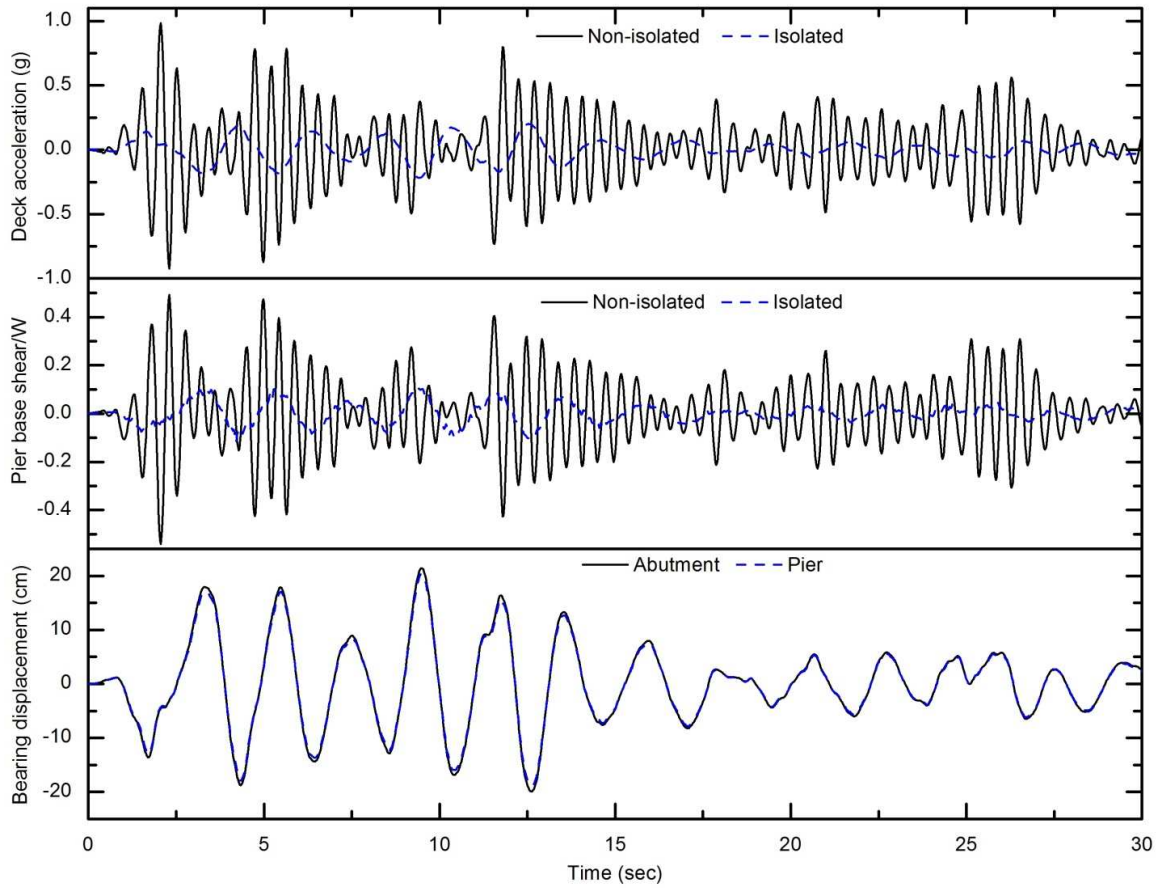


Figure 8.16 Time variation of the absolute deck acceleration, base shear in piers and bearing displacements in the transverse direction of the bridge to El-Centro, 1940 earthquake excitation ($T_b = 2$ sec and $\xi_b = 12.5\%$).

8.8 Modeling and Analysis of Base-Isolated Liquid Storage Tanks

Liquid storage tanks are very important structure, which is connected to social life. It has also wide applications in the industry. Apart from these applications it is strategically important since it is used for storage in the nuclear power plants. In past earthquakes there had been a number of reports on damage to liquid storage tanks. Therefore, it is necessary to design liquid storage tanks against earthquake. Figure 8.17 shows the schematic model of a typical liquid storage tank (refer Shriali and Jangid, 2002, 2003, Panchal and Jangid, 2008).

8.8.1 Assumptions

1. The entire liquid mass is assumed to have three components.
2. Masses are connected by corresponding equivalent springs.
3. Earthquake excitation imparted to the tank is unidirectional.

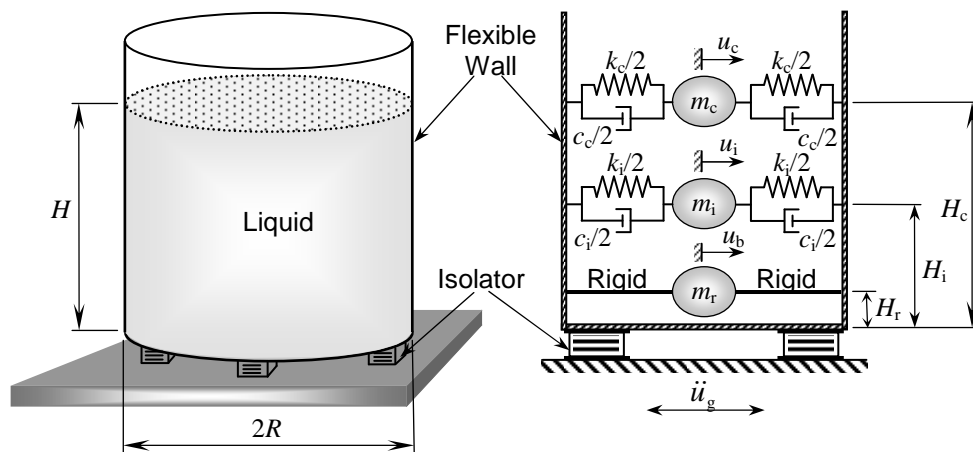


Figure 8.17 Model of base-isolated liquid storage tank.

8.8.2 Governing Equation of Motion

The mass components are convective, impulsive and rigid masses referred as m_c , m_i and m_r , respectively. The convective and impulsive masses are connected to the tank by corresponding equivalent springs. The system has three-degrees-of-freedom under unidirectional earthquake motion. These degrees-of-freedom are denoted by u_c , u_i and u_b , which denote the absolute displacement of convective, impulsive and rigid masses, respectively at each lumped mass. The parameters of the tanks considered are liquid height H , radius, R and average thickness of tank wall, t . The effective masses are defined in terms of total liquid mass, m from the parameters as

$$Y_c = 1.01327 - 0.87578S + 0.35708S^2 - 0.06692S^3 + 0.00439S^4 \quad (8.24)$$

$$Y_i = -0.15467 + 1.21716S - 0.62839S^2 + 0.14434S^3 - 0.0125S^4 \quad (8.25)$$

$$Y_r = -0.01599 + 0.86356S - 0.30941S^2 + 0.04083S^3 \quad (8.26)$$

where, $S = H/R$ is the ratio of the liquid height to radius of the tank; also known as aspect ratio, and Y_c , Y_i , and Y_r are the mass ratios defined as

$$Y_c = \frac{m_c}{m} \quad (8.27)$$

$$Y_i = \frac{m_i}{m} \quad (8.28)$$

$$Y_r = \frac{m_r}{m} \quad (8.29)$$

$$m = \pi R^2 H \rho_w \quad (8.30)$$

where, ρ_w is the mass density of liquid. The natural frequencies of sloshing mass, ω_c and impulsive mass, ω_i are given by following expressions,

$$\omega_i = \frac{P}{H} \sqrt{\frac{E}{\rho_s}} \quad (8.31)$$

$$\omega_c = \sqrt{1.84 \left(\frac{g}{R} \right) \tanh \left(1.84 \frac{H}{R} \right)} \quad (8.32)$$

where, E and ρ_s are the modulus of elasticity and density of tank wall, respectively; g is the acceleration due to gravity; and P is a dimensionless parameter expressed by

$$P = 0.07726 + 0.17563S - 0.106S^2 + 0.02609S^3 - 0.0025S^4 \quad (8.33)$$

The equations of motion of isolated liquid storage tank subjected to earthquake ground motion are expressed in the matrix form as

$$[m]\{\ddot{x}\} + [c]\{\dot{x}\} + [k]\{x\} = -[m]\{r\}\ddot{u}_g \quad (8.34)$$

where, $\{x\} = \{x_c, x_i, x_b\}^T$ is the displacement vector; $x_c = u_c - u_b$ is the displacement of the convective mass relative to bearing displacement; $x_i = u_i - u_b$ is the displacement of the impulsive mass relative to bearing displacement; $x_b = u_b - u_g$ is the displacement of the bearings relative to ground; $[m]$, $[c]$ and $[k]$ are the mass, damping and stiffness matrix of the system, respectively; $\{r\} = \{0 \ 0 \ 1\}^T$ is the influence coefficient vector; and \ddot{u}_g is the earthquake ground acceleration; and T indicates the transpose. The matrices $[m]$, $[c]$ and $[k]$ are expressed as

$$[m] = \begin{bmatrix} m_c & 0 & m_c \\ 0 & m_i & m_i \\ m_c & m_i & m_c + m_i + m_r \end{bmatrix} \quad (8.35)$$

$$[c] = \begin{bmatrix} c_c & 0 & 0 \\ 0 & c_i & 0 \\ 0 & 0 & c_b \end{bmatrix} \quad (8.36)$$

$$[k] = \begin{bmatrix} k_c & 0 & 0 \\ 0 & k_i & 0 \\ 0 & 0 & k_b \end{bmatrix} \quad (8.37)$$

where, c_c and c_i represent the damping and k_c and k_i represent the stiffness associated with the vibration of convective and impulsive masses of the storage tank while; c_b and k_b are the damping and stiffness of the isolation system, respectively. The response of the base-isolated tank can be obtained by solving the equation (8.34) using the step-by-step Newmark's Beta method given in the Section 7.5.

The equivalent stiffness and damping of the convective and impulsive masses are expressed as,

$$k_c = m_c \omega_c^2 \quad (8.38)$$

$$k_i = m_i \omega_i^2 \quad (8.39)$$

$$c_c = 2\xi_c m_c \omega_c \quad (8.40)$$

$$c_i = 2\xi_i m_i \omega_i \quad (8.41)$$

The damping and stiffness of the bearing are designed to provide the desired value of two parameters namely the period of isolation, T_b and bearing damping ratio, ξ_b expressed as

$$T_b = 2\pi \sqrt{\frac{m_c + m_i + m_r}{k_b}} \quad (8.42)$$

$$\xi_b = \frac{c_b}{2(m_c + m_i + m_r) \omega_b} \quad (8.43)$$

where, $\omega_b = 2\pi/T_b$ is the isolation frequency. The total base shear in the liquid storage tank, F_b , due to earthquake ground motion is expressed as

$$F_b = m_c \ddot{u}_c + m_i \ddot{u}_i + m_r \ddot{u}_b \quad (8.45)$$

Example 8.4

Consider a water storage tank with properties given below.

Type of Tank	$S (H/R)$	H (m)	t/R	ω_c (Hz)	ω_i (Hz)
Slender	1.85	11.3	0.004	0.273	5.963

The tank is considered as filled to a height, H with water. The damping ratios for convective mass and impulsive mass are taken as 0.5 per cent and 2 per cent, respectively. For the tank with steel wall the modulus of elasticity is taken as $E = 200$ MPa and the mass density, $\rho_s = 7,900$ kg/m³. The tank is isolated using the elastomeric bearings with $T_b = 2$ sec and $\xi_b = 10\%$. Determine the base shear, sloshing displacement, impulsive displacement and bearing displacement of the tank under El-Centro, 1940 earthquake motion.

Solution:

Based on the method developed in the Section 8.8, the computer program in the FORTRAN was written and the response of the tank to El-Centro, 1940 earthquake ground motion is shown in Figure 8.18. The maximum response of the bridge is summarized below:

Type of Tank	Non-isolated			Isolated			
	x_c (cm)	x_i (cm)	F_b/W	x_c (cm)	x_i (cm)	x_b (cm)	F_b/W
Slender	41.54	0.39	0.319	61.10	0.09	10.02	0.105

It is observed from the Figure 8.18 that the base shear and impulsive displacement of isolated tanks are significantly less in comparison to that without isolation system. Therefore, the isolation system is quite effective in reducing the base shear and impulsive displacement due earthquake ground motions. The peak bearing displacement for the tank is observed as 10.02 cm. The peak sloshing displacement as a result of seismic isolation is slightly increased.

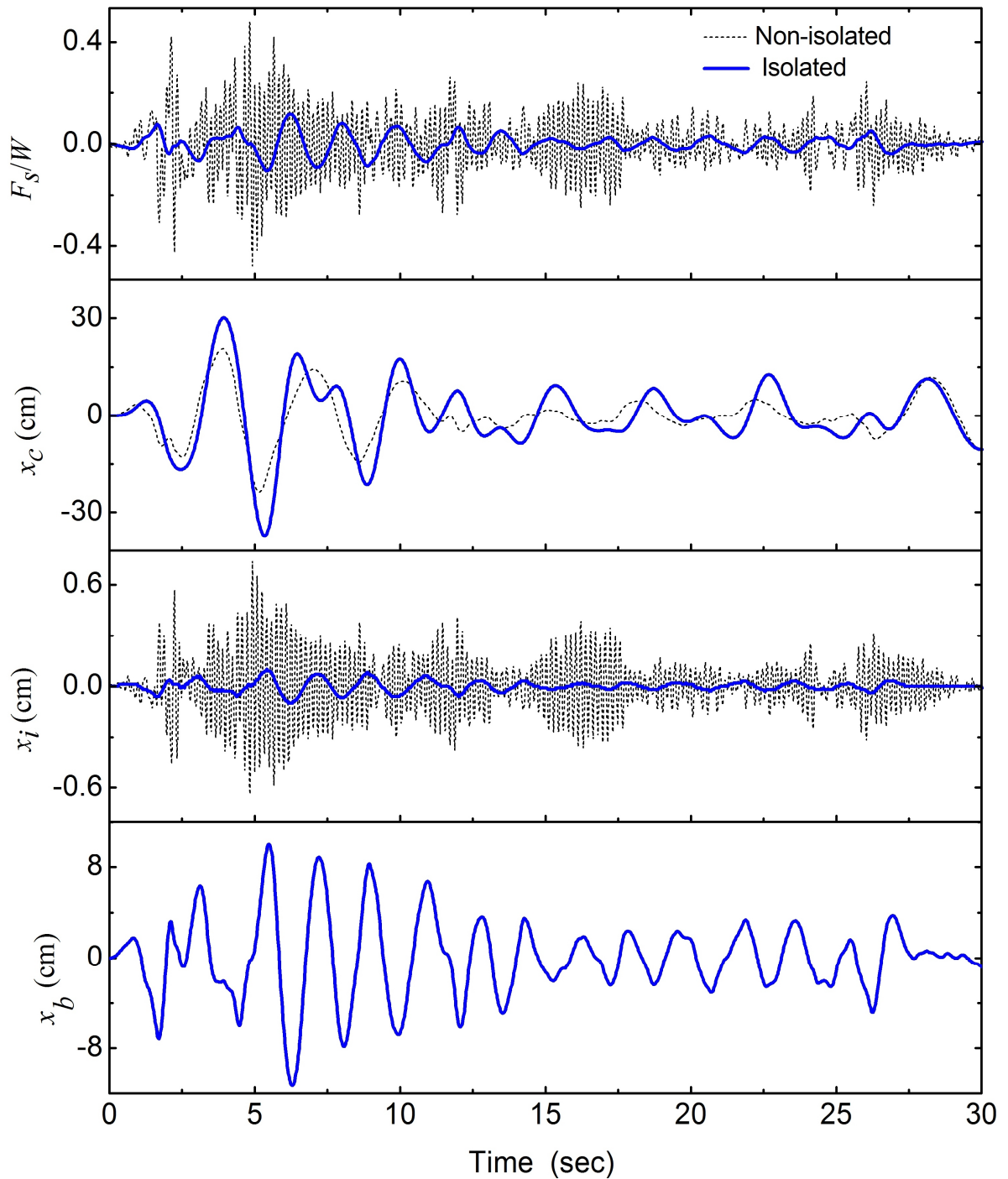


Figure 8.18 Time variation of the base shear, sloshing displacement, impulsive displacement and bearing displacement of the tank of Example 8.4.

8.9 Applications of Base Isolation

Base isolation was first formally used by Frank Lloyd Wright to design Imperial Hotel in Tokyo in 1921, though the technique then used is not prevalent as of today. Under the site, there was an 8 inch layer of fairly good soil, and below that, a layer of soft mud. This layer partially provided the necessary isolation from the horizontal ground movement during earthquake. The building was tied to the upper layer of good soil by closely spaced short piles that penetrated only as far as the top of the soft mud. The building performed extremely well in the devastating 1923 Tokyo earthquake.

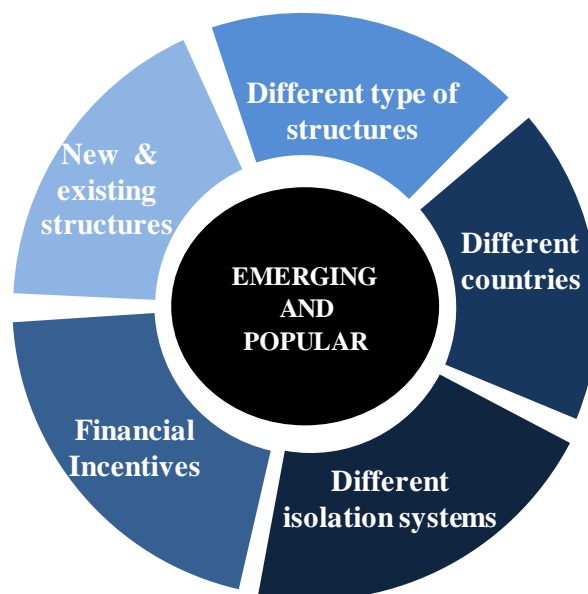


Figure 8.19 Rising popularity of base isolation method

Base isolation application as a means of earthquake mitigation is becoming a popular method. As depicted in Figure 8.19, ever since the base isolation was illustrated practically in 1909 by a medical doctor from Scarborough in England, the method became popular due to its simplicity, and its tremendous impact to mitigate damaging earthquake consequences. This method is used in new, and existing (as retrofit) structures, both important and civilian, in different type of structures and in different countries. From this simple concept, newer isolation system patents are often awarded, and some governments have also proposed financial incentives to reduce insurance premiums for the structures built utilizing these technologies as the confidence in its mitigation efforts are being proved.

Generally, the “old, traditionally-built” structures, such as the monuments and traditional buildings, are more affected by earthquakes. These buildings are mainly constructed in the

period before the ample use of reinforced concrete, with elements and technology based on the experience of the builders alone, without any structural-seismic design. Nevertheless, interesting construction techniques can be seen in these historical buildings throughout the pre-historic period up to the first half of the twentieth century. Therefore, increase on seismic performance of traditional-historical buildings is considered necessary, especially for those located in seismically active regions. The retrofitting by base isolation of such buildings becomes an obvious choice as the historical architectural characteristics of the building remains preserved (Matsagar and Jangid, 2008).

In bridges, the base isolation devices can rather easily be incorporated by replacing the traditional bridge bearings by isolation systems. Base isolation bearings serve the dual purpose of providing means for thermal movement as well as protecting the bridge from dynamic forces by increasing the fundamental time period, and dissipating the seismic energy by hysteretic damping.

Also, this method has started to be introduced in liquid storage tanks. Liquid storage tanks are lifeline structures, and strategically very important, since they have vital use in industries and nuclear power plants. Past earthquakes have demonstrated the seismic vulnerability of tanks wherein the damage occurred in the form of buckling of tank wall due to excessive development of compressive stresses, failure of piping systems, and uplift of anchorage system. The seismic behavior of liquid storage tanks is highly complex due to liquid-structure-interaction leading to a tedious design procedure from earthquake-resistant design point of view. Base isolation technique can be effectively used as retrofit scheme for liquid storage tanks as well.

Introduction of base isolation technique as means to mitigate earthquake in sensitive nuclear structures have got immense attention. It is mainly due to the fact that the provision of base isolators helps to maintain the standard design of nuclear structures which otherwise would escalate cost on relocation to different sites due to different seismic activities.

Different projects using base isolation technology are explained briefly to express its emerging and confident trend, country-wise. It is not possible to enlist all cases of base-isolated structures, however a few projects that sufficiently state its emergence and popularity is discussed. The details of some of the base-isolated projects are presented in Appendix-IV.

In the United States of America (USA), Foothill Communities Law and Justice Center, County of San Bernardino, California was the first newly constructed building in 1986 in the United States applied with base isolation technology. The building is a five story plus

basement braced steel frame supported on 98 high-damping rubber bearings. It is located near to one of the most active San Francisco faults. Some of the systems installed were removed and tested as part of long term monitoring, and were found to perform satisfactorily (Clark et al., 1997). The Oakland City Hall, built in 1914 is one of the most noted retrofitted old structures utilizing base isolation technology. This nineteen stories high and 97.5 m tall building has a full basement, a three-story podium, a ten-story office tower, and a two storied base for the clock tower that is itself 26.5 m high. The structure of the building is a riveted steel frame with infill masonry walls of brick, granite and terracotta. The isolation system uses a combination of 36 lead rubber bearings, and 75 ordinary rubber bearings. The bearings range from 737 mm to 940 mm in diameter, and are 445 mm tall. A moat was constructed around the building to provide a seismic gap of 508 mm to avoid impounding (Walters, 2003). The City Halls such as Los Angeles, San Francisco and historical building Utah State Capitol are the important base isolation projects. The Golden Gate Bridge North was built in 1973, however the proximity of the bridge to the San Andreas Fault places it at risk for a significant earthquake. Once, this bridge was thought to have been able to withstand any magnitude of anticipated earthquake, however, it was actually vulnerable to complete structural failure triggered by the failure of the supports on the 320 feet (98 m) arch over fort point. A \$392 million program was initiated to improve the structure's ability to withstand such an event with only minimal (repairable) damage. The retrofit program, using lead rubber bearings, is planned to be completed date in 2012. In New Zealand, William Clayton Building was the first building to be built using lead rubber base isolation system in 1970. The idea of introducing central lead plug to rubber bearing was first used in this building to increase the damping up to 10-15% of the critical damping. The building is four-storied high, and has a reinforced concrete frame. The natural period of the isolated building is 2.5 seconds. The building sits on 80 LRBs. Later in 1995, energy dampers were introduced to compensate for the small seismic gaps that were provided earlier due to less understanding of ground motion variations at that time (Robinson, 2000). The function and heritage of the New Zealand Parliament Building constructed in 1922 were crucial criteria for its protection using base isolation system. The building consists of five stories of unreinforced masonry bearing walls supporting concrete floors totaling 70,000 sq. m of floor area. A total of 417 high damping rubber (HDR), and lead rubber bearings (LRB) were installed between the foundations and the superstructure. The retrofit involved re-piling the building with lead-rubber bearings and rubber bearings in the supports, as well as cutting a seismic gap in the 500 mm thick concrete walls. During an earthquake the building will be able to move in any

direction on a horizontal plane up to distances of 300 mm (Robinson, 2000).

Museum of New Zealand-Te Papa is a structure on the Waterfront in Central Wellington. Te Papa is believed to be the heaviest seismically isolated building in the world. This 190×104 m building, with a triangular floor plan, is isolated by 142 lead-rubber bearings with Teflon sliding bearings under the shear walls. The museum with five floor levels has a total floor area of 35,000 sq. m, and height of 23 m. The building was not designed according to code, however it is required to suffer no damage in a 250 year return period earthquake, and not collapse with a 2000 year earthquake (Robinson, 2000).

In Japan, the isolation performance of the base-isolated computer center of the Ministry of Post and Telecommunications. The superstructure of the steel reinforced concrete structure has six stories, and a total floor area of 46,823 sq. m. The seismic isolation system in this building, considered as the largest base-isolated building in the world, comprises of 54 lead-rubber bearings.

In India, the first base isolation project in India was completed for a hospital in 2003. The three hundred bed, 4-storied, Bhuj hospital (Figure 8.20) replaces the old hospital building that claimed 176 lives when it collapsed during the major 26th January 2001 Bhuj earthquake. The isolation system comprises of 280 lead-rubber and sliding bearings developed using technology in New Zealand (Sharpe, 2002).



Figure 8.20 Bhuj Hospital (Source: Science Learn - <http://www.sciencelearn.org.nz/Contexts/Earthquakes/Sci-Media/Images/Bhuj-Hospital>).

As of 2005, there are six seismically isolated nuclear power plants; four in France, and two in South Africa (Malushte and Whittaker, 2005). At the Cruas plant in France, each of

the four units has been constructed on 1,800 neoprene pads measuring 500×500×65 mm. The seismicity at the site is moderate with a safe shutdown earthquake design acceleration of 0.2g (g is gravitational acceleration). In Koeberg, South Africa, two units are isolated on a total of 2,000 neoprene pads measuring 700×700×100 mm. For this site, the safe shutdown earthquake design acceleration is 0.3g. The pads are outfitted with flat sliders on the top surface, consisting of a lead-bronze alloy lower plate, and a polished stainless steel upper plate.

8.10 Tutorial Problems

- Q1. Determine the horizontal and vertical stiffness of square (200mm×200mm) and circular (diameter = 200mm) having height between top and bottom steel plate as 50mm. The five number of 3mm thick steel plates are provided in the each bearing. Take the shear modulus of the rubber as 0.9 N/mm².
- Q2. Consider a three-story base-isolated building modeled as 4-DOF system and rigid floors as shown in Figure 8.21 with fixed base and isolated condition. Take the inter-story lateral stiffness of floors i.e. $k_1 = k_2 = k_3 = 16357.5$ kN/m and the floor & base mass $m_b = m_1 = m_2 = 10000$ kg and $m_3 = 5000$ kg. The above building is isolated by the elastomeric bearings with $T_b = 2$ sec and $\xi_b = 0.1$. Determine the maximum top floor absolute acceleration and isolator displacement due to El-Centro, 1940 earthquake ground motion.

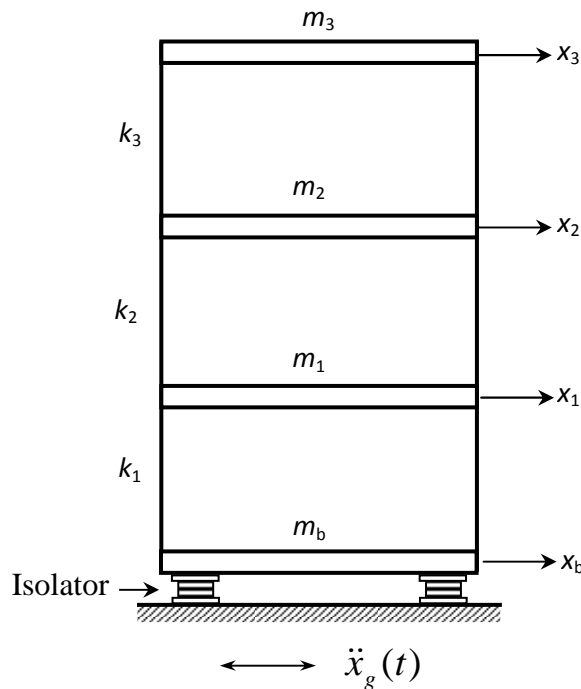


Figure 8.21 Model of fixed base and base isolated building.

- Q3. If the building of Q2 is to be isolated by lead-rubber bearings with $T_b = 2$ sec, $F_y/W = 0.05$ and $\xi_b = 0.1$, determine the maximum top floor absolute acceleration and isolator displacement due to El-Centro, 1940 earthquake ground motion.
- Q4. Let the building of Q2 be isolated by FPS system with $T_b = 2$ sec and $\mu = 0.05$. Determine the maximum top floor absolute acceleration and isolator displacement due to El-Centro, 1940 earthquake ground motion.

Q5. Consider a two-span continuous bridge with properties of deck and piers given below.

Properties	Deck	Piers
Cross-sectional area (m ²)	4	3
Moment of inertia as (m ⁴)	2	0.8
Modulus of elasticity (N/m ²)	25×10 ⁹	25×10 ⁹
Mass density (kg/m ³)	2.4×10 ³	2.4×10 ³
Length/height (m)	2@25 = 50	6

The bridge is isolated using the elastomeric bearings with $T_b = 2$ sec and $\xi_b = 10\%$. Determine the absolute acceleration at the center of bridge deck and the relative displacement of the bearings in the longitudinal direction under the El-Centro, 1940 earthquake motion.

Q6. Consider a water storage tank with properties given below.

Type of Tank	$S (H/R)$	H (m)	t/R	ω_c (Hz)	ω_t (Hz)
Broad	0.60	14.6	0.004	0.123	3.944

The tank is considered as filled to a height, H with water. The damping ratios for convective mass and impulsive mass are taken as 0.5 per cent and 2 per cent, respectively. For the tank with steel wall the modulus of elasticity is taken as $E = 200$ MPa and the mass density, $\rho_s = 7,900$ kg/m³. The tank is isolated using the elastomeric bearings with $T_b = 2$ sec and $\xi_b = 10\%$. Determine the base shear, sloshing displacement, impulsive displacement and bearing displacement of the tank under El-Centro, 1940.

8.11 Solution of Tutorial Problems

1.

Bearing Shape	K_v (N/mm)	K_h (N/mm)
Square	692228.6	1028.6
Circular	484702.8	807.8

2. Top floor absolute acceleration = 1.3m/sec^2 and isolator displacement = 0.12m

3. Top floor absolute acceleration = 2.04m/sec^2 and isolator displacement = 0.066m

4. Top floor absolute acceleration = 3.35m/sec^2 and isolator displacement = 0.057m

5. Absolute deck acceleration = 1.2m/sec^2 and isolator displacement = 0.117m

6.

Type of Tank	Non-isolated			Isolated			
	x_c (cm)	x_i (cm)	F_b/W	x_c (cm)	x_i (cm)	x_b (cm)	F_b/W
Broad	53.08	1.28	0.258	57.41	0.22	7.71	0.079